ARTICLES
PUBLISHED ONLINE: 13 FEBRUARY 2011 | DOI: 10.1038/NPHYS1915
nature physics

Non-Abelian statistics and topological quantum information processing in 1D wire networks

Jason Alicea[1]*, Yuval Oreg[2], Gil Refael[3], Felix von Oppen[4] and Matthew P. A. Fisher[3,5]

The synthesis of a quantum computer remains an ongoing challenge in modern physics. Whereas decoherence stymies most approaches, topological quantum computation schemes evade decoherence at the hardware level by storing quantum information non-locally. Here we establish that a key operation—braiding of non-Abelian anyons—can be implemented using one-dimensional semiconducting wires. Such wires can be driven into a topological phase supporting long-sought particles known as Majorana fermions that can encode topological qubits. We show that in wire networks, Majorana fermions can be meaningfully braided by simply adjusting gate voltages, and that they exhibit non-Abelian statistics like vortices in a $p+ip$ superconductor. We propose experimental set-ups that enable probing of the Majorana fusion rules and the efficient exchange of arbitrary numbers of Majorana fermions. This work should open a new direction in topological quantum computation that benefits from physical transparency and experimental feasibility.

The experimental realization of a quantum computer ranks among the foremost outstanding goals in physics and has traditionally been hampered by decoherence. In this regard topological quantum computing holds considerable promise, as here one embeds quantum information in a non-local, intrinsically decoherence-free fashion[1–6]. A toy model of a spinless, two-dimensional (2D) $p+ip$ superconductor nicely illustrates the key ideas. Vortices in such a state bind exotic particles known as Majorana fermions, which cost no energy and therefore generate ground state degeneracy. Because of the Majoranas, vortices exhibit non-Abelian braiding statistics[7–11]: adiabatically exchanging vortices noncommutatively transforms the system from one ground state to another. Quantum information encoded in this ground state space can be controllably manipulated by braiding operations—something the environment finds difficult to achieve.

Despite this scheme's elegance, finding suitable 'hardware' poses a serious challenge. Although most effort has focused on the quantum Hall state at filling fraction[10,12] $\nu=5/2$, numerous realistic alternative routes to generating non-Abelian topological phases have recently appeared[13–20]. Among these, two groups[21,22] recognized that one-dimensional (1D) semiconducting wires can be engineered, relatively easily, into Kitaev's[23] topological superconducting state supporting Majorana fermions. Motivated by this exciting possibility, we examine the prospect of exploiting 1D wires for topological quantum computation.

The suitability of 1D wires for this purpose is far from obvious. Manipulating, braiding, and realizing non-Abelian statistics of Majorana fermions are all central to topological quantum computation (although measurement-only approaches sidestep the braiding requirement[5]). Whereas Majorana fermions can be transported, created, and fused by gating a wire, braiding and non-Abelian statistics pose serious puzzles. Indeed, braiding statistics is ill-defined in 1D because particles inevitably 'collide' during an exchange. This problem can be surmounted in wire networks, the simplest being a T-junction formed by two perpendicular wires. Even in such networks, however, non-Abelian statistics does not immediately follow, as recognized by Wimmer and colleagues[24]. For example, non-Abelian statistics in a 2D $p+ip$ superconductor is intimately linked to vortices binding the Majoranas[10,11]. We demonstrate that, despite the absence of vortices, Majorana fermions in semiconducting wires exhibit non-Abelian statistics and transform under exchange exactly like vortices in a $p+ip$ superconductor.

We further propose experimental setups ranging from minimal circuits (involving one wire and a few gates) for probing the Majorana fusion rules, to scalable networks that permit efficient exchange of many Majoranas. The 'fractional Josephson effect'[13,21–23,25], along with Hassler *et al.*'s recent proposal[26] enable qubit readout in this setting. The relative ease with which Majorana fermions can be stabilized in 1D wires, combined with the physical transparency of their manipulation, render these set-ups extremely promising topological quantum information processing platforms. Although braiding of Majoranas alone does not permit universal quantum computation[6,27–30], implementation of these ideas would constitute a critical step towards this ultimate goal.

Majorana fermions in 1D wires

We begin by discussing the physics of a single wire. Valuable intuition can be garnered from Kitaev's toy model for a spinless, p-wave superconducting N-site chain[23]:

$$H=-\mu\sum_{x=1}^{N}c_x^{\dagger}c_x-\sum_{x=1}^{N-1}(tc_x^{\dagger}c_{x+1}+|\Delta|e^{i\phi}c_xc_{x+1}+h.c.) \qquad (1)$$

where c_x is a spinless fermion operator and μ, $t>0$, and $|\Delta|e^{i\phi}$ respectively denote the chemical potential, tunnelling strength, and pairing potential. The bulk- and end-state structure becomes particularly transparent in the special case[23] $\mu=0$, $t=|\Delta|$. Here it is useful to express

$$c_x=\frac{1}{2}e^{-i(\phi/2)}(\gamma_{B,x}+i\gamma_{A,x}) \qquad (2)$$

with $\gamma_{\alpha,x}=\gamma_{\alpha,x}^{\dagger}$ Majorana fermion operators satisfying $\{\gamma_{\alpha,x},\gamma_{\alpha',x'}\}=2\delta_{\alpha\alpha'}\delta_{xx'}$. These expressions expose the defining

[1]Department of Physics and Astronomy, University of California, Irvine, California 92697, USA, [2]Department of Condensed Matter Physics, Weizmann Institute of Science, Rehovot, 76100, Israel, [3]Department of Physics, California Institute of Technology, Pasadena, California 91125, USA, [4]Dahlem Center for Complex Quantum Systems and Fachbereich Physik, Freie Universität Berlin, 14195 Berlin, Germany, [5]Department of Physics, University of California, Santa Barbara, California 93106, USA. *e-mail: aliceaj@uci.edu.

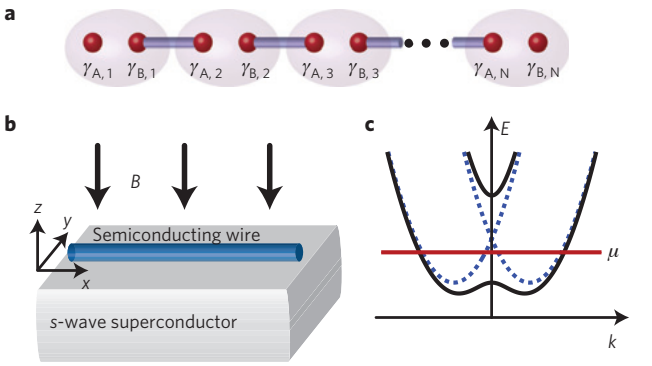

Figure 1 | Majorana fermions appear at the ends of a 1D 'spinless' *p*-wave superconductor, which can be experimentally realized in semiconducting wires[21,22]. **a**, Pictorial representation of the ground state of equation (1) in the limit $\mu = 0$, $t = |\Delta|$. Each spinless fermion in the chain is decomposed in terms of two Majorana fermions $\gamma_{A,x}$ and $\gamma_{B,x}$. Majoranas $\gamma_{B,x}$ and $\gamma_{A,x+1}$ combine to form an ordinary, finite-energy fermion, leaving two zero-energy end Majoranas $\gamma_{A,1}$ and $\gamma_{B,N}$ as shown[23]. **b**, A spin–orbit-coupled semiconducting wire deposited on an *s*-wave superconductor can be driven into a topological superconducting state exhibiting such end Majorana modes by applying an external magnetic field[21,22]. **c**, Band structure of the semiconducting wire when $\mathbf{B} = 0$ (dashed lines) and $\mathbf{B} \neq 0$ (solid lines). When μ lies in the band gap generated by the field, pairing inherited from the proximate superconductor drives the wire into the topological state.

characteristics of Majorana fermions—they are their own antiparticle and constitute 'half' of an ordinary fermion. In this limit the Hamiltonian becomes

$$H = -it\sum_{x=1}^{N-1}\gamma_{B,x}\gamma_{A,x+1}$$

Consequently, $\gamma_{B,x}$ and $\gamma_{A,x+1}$ combine to form an ordinary fermion $d_x = (\gamma_{A,x+1} + i\gamma_{B,x})/2$, which costs energy $2t$, reflecting the wire's bulk gap. Conspicuously absent from H, however, are $\gamma_{A,1}$ and $\gamma_{B,N}$, which represent end-Majorana modes. These can be combined into an ordinary (although highly non-local) zero-energy fermion $d_{end} = (\gamma_{A,1} + i\gamma_{B,N})/2$. Thus there are two degenerate ground states which serve as topologically protected qubit states: $|0\rangle$ and $|1\rangle = d_{end}^{\dagger}|0\rangle$, where $d_{end}|0\rangle = 0$. Figure 1a illustrates this physics pictorially.

Away from this limit the Majorana end states no longer retain this simple form, but survive provided the bulk gap remains finite[23]. This occurs when $|\mu| < 2t$, where a partially filled band pairs. The bulk gap closes when $|\mu| = 2t$. For larger $|\mu|$, pairing occurs in a fully occupied or vacant band, and a trivial superconducting state without Majoranas emerges.

Realizing Kitaev's topological superconducting state experimentally requires a 'spinless' system (that is, with one pair of Fermi points) that *p*-wave pairs at the Fermi energy. Both criteria can be satisfied in a spin–orbit-coupled semiconducting wire deposited on an *s*-wave superconductor by applying a magnetic field[21,22] (see Fig. 1b). The simplest Hamiltonian describing such a wire reads

$$\mathcal{H} = \int \mathrm{d}x\left[\psi_x^{\dagger}\left(-\frac{\hbar^2\partial_x^{\,2}}{2m} - \mu - i\hbar u\hat{\mathbf{e}}\cdot\boldsymbol{\sigma}\partial_x - \frac{g\mu_B B_z}{2}\sigma^z\right)\psi_x + (|\Delta|\mathrm{e}^{i\varphi}\psi_{\downarrow x}\psi_{\uparrow x} + h.c.)\right] \quad (3)$$

The operator $\psi_{\alpha x}$ corresponds to electrons with spin α, effective mass m, and chemical potential μ. (We suppress the spin indices except in the pairing term.) In the third term, u denotes the spin–orbit[31,32] strength, and $\boldsymbol{\sigma} = (\sigma^x, \sigma^y, \sigma^z)$ is a vector of Pauli matrices. This coupling favours aligning spins along or against the unit vector $\hat{\mathbf{e}}$, which we assume lies in the (x, y) plane. The fourth term represents the Zeeman coupling due to the magnetic field $B_z < 0$. Note that spin–orbit enhancement can lead[33] to $g \gg 2$. Finally, the last term reflects the spin-singlet pairing inherited from the superconductor by means of the proximity effect.

To understand the physics of equation (3), consider first $B_z = \Delta = 0$. The dashed lines in Fig. 1c illustrate the band structure here—clearly no 'spinless' regime is possible. Introducing a magnetic field generates a band gap $\propto |B_z|$ at zero momentum, as the solid line in Fig. 1c depicts. When μ lies in this gap the system exhibits a single pair of Fermi points as desired. Turning on Δ weakly compared to the gap then effectively *p*-wave pairs fermions in the lower band with momentum k and $-k$, driving the wire into Kitaev's topological phase[21,22]. (Singlet pairing in equation (3) generates *p*-wave pairing because spin–orbit coupling favours opposite spins for k and $-k$ states.) Quantitatively, realizing the topological phase requires[21,22] $|\Delta| < g\mu_B|B_z|/2$, which we hereafter assume holds. The opposite limit $|\Delta| > g\mu_B|B_z|/2$ effectively violates the 'spinless' criterion because pairing strongly intermixes states from the upper band, producing an ordinary superconductor without Majorana modes.

In the topological phase, the connection to equation (1) becomes more explicit when $g\mu_B|B_z| \gg mu^2, |\Delta|$ where the spins nearly polarize. One can then project equation (3) onto a simpler one-band problem by writing $\psi_{\uparrow x} \sim (u(e_y + ie_x)/g\mu_B|B_z|)\partial_x\Psi_x$ and $\psi_{\downarrow x} \sim \Psi_x$, with Ψ_x the lower-band fermion operator. To leading order, one obtains

$$\mathcal{H}_{\mathrm{eff}} \sim \int \mathrm{d}x\left[\Psi_x^{\dagger}\left(-\frac{\hbar^2\partial_x^{\,2}}{2m} - \mu_{\mathrm{eff}}\right)\Psi_x + \left(|\Delta_{\mathrm{eff}}|\mathrm{e}^{i\varphi_{\mathrm{eff}}}\Psi_x\partial_x\Psi_x + h.c.\right)\right] \quad (4)$$

where $\mu_{\mathrm{eff}} = \mu + g\mu_B|B_z|/2$ and the effective *p*-wave pair field reads

$$|\Delta_{\mathrm{eff}}|\mathrm{e}^{i\varphi_{\mathrm{eff}}} \approx \frac{u|\Delta|}{g\mu_B|B_z|}\mathrm{e}^{i\varphi}(e_y + ie_x) \quad (5)$$

The dependence of φ_{eff} on $\hat{\mathbf{e}}$ will be important below when we consider networks of wires. Equation (4) constitutes an effective low-energy Hamiltonian for Kitaev's model in equation (1) in the low-density limit. From this perspective, the existence of end-Majoranas in the wire becomes manifest. We exploit this correspondence below when addressing universal properties such as braiding statistics, which must be shared by the topological phases described by equation (3) and the simpler lattice model, equation (1).

We now seek a practical method to manipulate Majorana fermions in the wire. As motivation, consider applying a gate voltage to adjust μ uniformly across the wire. The excitation gap obtained from equation (3) at $k = 0$ varies with μ as

$$E_{\mathrm{gap}}(k=0) = \left|\frac{g\mu_B|B_z|}{2} - \sqrt{|\Delta|^2 + \mu^2}\right|$$

For $|\mu| < \mu_c = \sqrt{(g\mu_B B_z/2)^2 - |\Delta|^2}$ the topological phase with end Majoranas emerges, whereas for $|\mu| > \mu_c$ a topologically trivial phase appears. A uniform gate voltage thus allows the creation or removal of the Majorana fermions. However, when $|\mu| = \mu_c$ the bulk gap closes, and the excitation spectrum at small momentum behaves as $E_{\mathrm{gap}}(k) \approx \hbar v|k|$, with velocity $v = 2u|\Delta|/(g\mu_B|B_z|)$. The gap closure is clearly undesirable, as we would like to manipulate Majorana fermions without generating further quasiparticles.

This problem can be circumvented by employing a 'keyboard' of locally tunable gates as in Fig. 2, each impacting μ over a finite

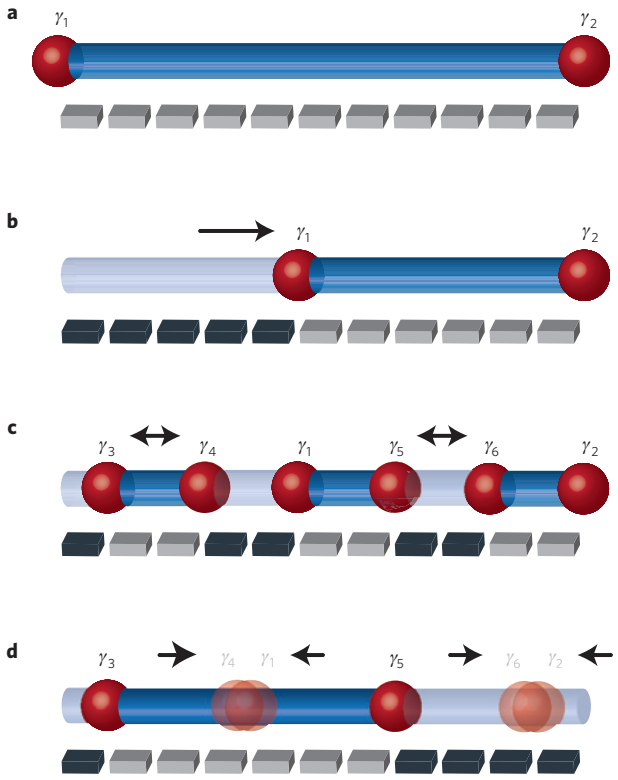

Figure 2 | Applying a 'keyboard' of individually tunable gates to the wire allows local control of which regions are topological (dark blue) and non-topological (light blue), and hence manipulate Majorana fermions while maintaining the bulk gap. As **a** and **b** illustrate, sequentially applying the leftmost gates drives the left end of the wire non-topological, thereby transporting γ_1 rightward. Nucleating a topological section of the wire from an ordinary region or vice versa creates pairs of Majorana fermions out of the vacuum as in **c**. Similarly, removing a topological region entirely or connecting two topological regions as sketched in **d** fuses Majorana fermions into either the vacuum or a finite-energy quasiparticle.

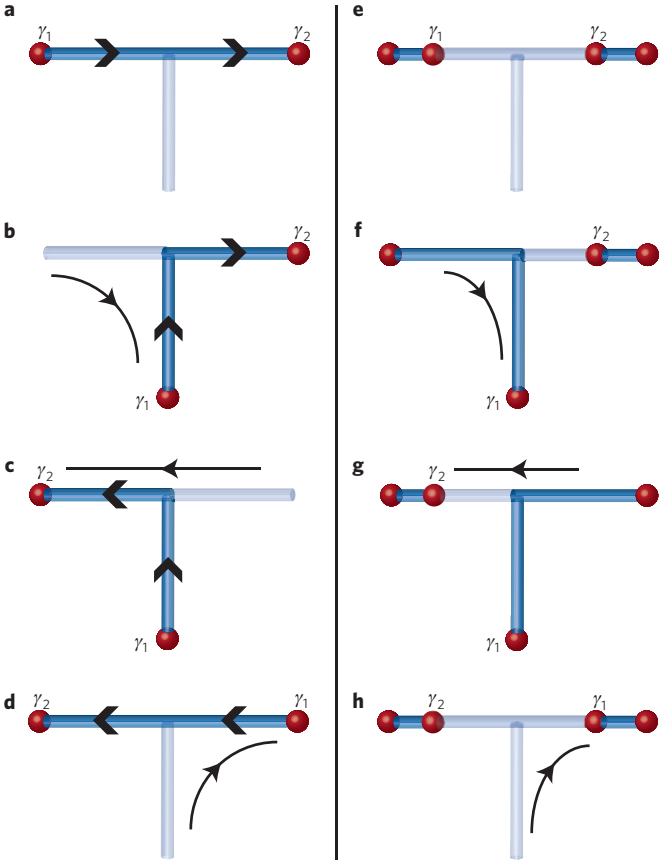

Figure 3 | A T-junction provides the simplest wire network that enables meaningful adiabatic exchange of Majorana fermions. Using the methods of Fig. 2, one can braid Majoranas bridged by either a topological region (dark blue lines) as in **a**–**d**, or a non-topological region (light blue lines) as in **e**–**h**. The arrows along the topological regions in **a**–**d** are useful for understanding the non-Abelian statistics, as outlined in the main text.

length $L_{\rm gate}$ of the wire. When a given gate locally tunes the chemical potential across $|\mu| = \mu_c$, a finite excitation gap $E_{\rm gap} \sim \hbar v\pi/L_{\rm gate}$ remains. (Roughly, the gate creates a potential well that supports only k larger than $\sim\pi/L_{\rm gate}$.) Assuming $g\mu_B|B_z|/2 \sim 2|\Delta|$ and $\hbar u \sim 0.1\,{\rm eV\,\AA}$ yields a velocity $v \sim 10^4\,{\rm m\,s^{-1}}$; the gap for a 0.1 μm wide gate is then of order 1 K. We consider this a conservative estimate—heavy-element wires such as InSb and/or narrower gates could generate substantially larger gaps.

Local gates allow Majorana fermions to be transported, created, and fused, as outlined in Fig. 2. As one germinates pairs of Majorana fermions, the ground state degeneracy increases, as does our capacity to topologically store quantum information. Specifically, $2n$ Majoranas generate n ordinary zero-energy fermions, with occupation numbers that specify topological qubit states. Adiabatically braiding the Majorana fermions to manipulate these qubits, however, is impossible in a single wire. Thus we now turn to the simplest arrangement permitting exchange—the T-junction of Fig. 3.

Majorana braiding and non-Abelian statistics

First, we explore the properties of the junction where the wires in Fig. 3 meet (see the Supplementary Information for more details). It is instructive to view the T-junction as three segments meeting at a point. When only one segment realizes a topological phase, a single zero-energy Majorana fermion exists at the junction. When two topological segments meet at the junction, as in Fig. 3a and b, generically no Majorana modes exist there. To see this, imagine decoupling the topological segments so that two nearby Majorana modes exist at the junction; restoring the coupling generically combines these Majoranas into an ordinary, finite-energy fermion.

As an illustrative example, consider the setup of Fig. 3a and model the left and right topological segments by Kitaev's model with $\mu = 0$ and $t = |\Delta|$ in equation (1). (For simplicity we exclude the non-topological vertical wire in Fig. 3a.) Suppose furthermore that $\phi = \phi_{\rm L/R}$ in the left/right chains and that the fermion $c_{{\rm L},N}$ at site N of the left chain couples weakly to the fermion $c_{{\rm R},1}$ at site 1 of the right chain via $H_\Gamma = -\Gamma(c_{{\rm L},N}{}^\dagger c_{{\rm R},1} + h.c.)$. Using equation (2), the Majoranas at the junction couple as follows,

$$H_\Gamma \sim -\frac{i\Gamma}{2}\cos\left(\frac{\phi_{\rm L}-\phi_{\rm R}}{2}\right)\gamma^{\rm L}_{{\rm B},N}\gamma^{\rm R}_{{\rm A},1} \qquad (6)$$

and therefore generally combine into an ordinary fermion[23]. An exception occurs when the regions form a π-junction—that is, when $\phi_{\rm L} - \phi_{\rm R} = \pi$—which fine-tunes their coupling to zero. Importantly, coupling between end Majoranas in the semiconductor context is governed by the same $\phi_{\rm L} - \phi_{\rm R}$ dependence as in equation (6) (refs 21,22).

Finally, when three topological segments meet, again only a single Majorana mode exists at the junction without fine-tuning. Three Majorana modes appear only when all pairs of wires simultaneously form mutual π junctions (which is possible because the superconducting phases are defined with respect to a direction in each wire; see the Supplementary Information).

Recall from equation (5) that the spin orientation favoured by spin–orbit coupling determines the effective superconducting phase of the semiconducting wires. Two wires at right angles to one another therefore exhibit a $\pi/2$ phase difference, well away from the pathological limits mentioned above. One can thus always transport Majorana fermions across the junction without generating spurious zero-modes.

T-junctions allow exchange of Majoranas residing on either the same or different topological regions. Figure 3a–d illustrates a counterclockwise braid for the former case, whereas Fig. 3e–h illustrates the latter. Although the Majoranas can now be exchanged, their non-Abelian statistics remains to be proven. Let us first recall how non-Abelian statistics of vortices arises in a spinless 2D $p+ip$ superconductor[10,11]. Ultimately, this can be deduced by considering two vortices which bind Majorana fermions γ_1 and γ_2. As the spinless fermion operators effectively change sign on advancing the superconducting phase by 2π, one introduces branch cuts emanating from the vortices; crucially, a Majorana fermion changes sign whenever crossing such a cut. On exchanging the vortices, γ_2 (say) crosses the branch cut emanating from the other vortex, leading to the transformation rule $\gamma_1 \to \gamma_2$ and $\gamma_2 \to -\gamma_1$, which is generated by the unitary operator $U_{12} = \exp(\pi\gamma_2\gamma_1/4)$. With many vortices, the analogous unitary operators U_{ij} implementing exchange of γ_i and γ_j do not generally commute, implying non-Abelian statistics.

Following an approach similar to Stern and colleagues[34], we now argue that Majorana fermions in wires transform exactly like those bound to vortices under exchange, and hence also exhibit non-Abelian statistics. This can be established most simply by considering the exchange of two Majorana fermions γ_1 and γ_2, as illustrated in Fig. 3a–d. At each step of the exchange, there are two degenerate ground states $|0\rangle$ and $|1\rangle = f^\dagger|0\rangle$, where $f = (\gamma_1 + i\gamma_2)/2$ annihilates $|0\rangle$. In principle, one can deduce the transformation rule from the Berry phases $\chi_n \equiv \mathrm{Im}\int \mathrm{d}t\,\langle n|\partial_t|n\rangle$ acquired by the many-body ground states $|n\rangle = |0\rangle$ and $|1\rangle$, although in practice these are hard to evaluate.

As exchange statistics is a universal property, however, we are free to deform the problem to our convenience provided the energy gap remains finite. As a first simplification, because the semiconductor Hamiltonian and Kitaev's model in equation (1) can be smoothly connected, let us consider the case where each wire in the T-junction is described by the latter. More importantly, we further deform Kitaev's Hamiltonian to be purely real as we exchange $\gamma_{1,2}$. The states $|0\rangle$ and $|1\rangle$ can then also be chosen real, leading to an enormous simplification: although these states still evolve nontrivially the Berry phase accumulated during this evolution vanishes.

For concreteness, we deform the Hamiltonian such that $\mu < 0$ and $t = \Delta = 0$ in the non-topological regions of Fig. 3. For the topological segments, reality implies that the superconducting phases must be either 0 or π. It is useful to visualize the sign choice for the pairing with arrows as in Fig. 3. (To be concrete, we take the pairing $|\Delta|e^{i\phi}c_jc_{j+1}$ such that the site indices increase moving rightward/upward in the horizontal/vertical wires; the case $\phi = 0$ then corresponds to rightward/upward arrows, whereas leftward/downward arrows indicate $\phi = \pi$.) To avoid generating π junctions, when two topological segments meet at the junction, one arrow must point into the junction while the other must point out. With this simple rule in mind, we see in Fig. 3 that although we can successfully swap the Majoranas while keeping the Hamiltonian real, we inevitably end up reversing the arrows along the topological region. In other words, the sign of the pairing has flipped relative to our initial Hamiltonian.

To complete the exchange we must then perform a gauge transformation which restores the Hamiltonian to its original form. This can be accomplished by multiplying all fermion creation operators by i; in particular, $f^\dagger = (\gamma_1 - i\gamma_2)/2 \to if^\dagger = (\gamma_2 + i\gamma_1)/2$. It follows that $\gamma_1 \to \gamma_2$ and $\gamma_2 \to -\gamma_1$, which the unitary transformation

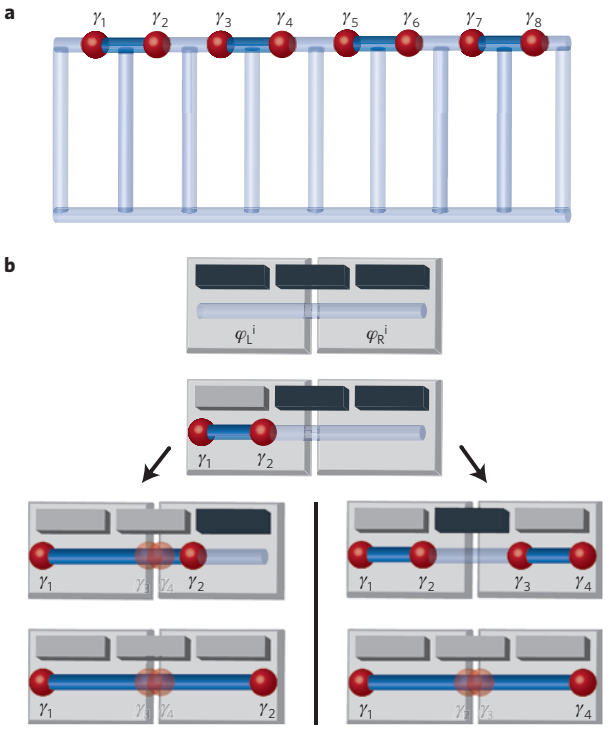

Figure 4 | Experimental set-ups that allow the probing of non-Abelian statistics and Majorana-fermion fusion rules. a, Example of a semiconductor wire network which allows for efficient exchange of many Majorana fermions. Adjacent Majoranas can be exchanged as in Fig. 3, whereas non-adjacent Majoranas can be transported to the lower wire to be similarly exchanged. **b**, Minimal set-up designed to detect the non-trivial Majorana fusion rules. Majoranas $\gamma_{1,2}$ are first created out of the vacuum. In the left path, γ_2 is shuttled rightward, and Majoranas $\gamma_{3,4}$ always combine to form a finite-energy state which is unoccupied. In the right path, $\gamma_{3,4}$ are also created out of the vacuum, and then γ_2 and γ_3 fuse with 50% probability into either the vacuum or a finite-energy quasiparticle. The Josephson current flowing across the junction allows the deduction of the presence or absence of this extra quasiparticle.

$U_{12} = \exp(\pi\gamma_2\gamma_1/4)$ generates as in the 2D $p+ip$ case. (Note that one could alternatively multiply all fermion creation operators by $-i$ instead of i to change the sign of the pairing, which would lead to the slightly different transformation $\gamma_1 \to -\gamma_2$ and $\gamma_1 \to \gamma_2$. The ambiguity disappears if one exchanges the Majoranas while keeping the superconducting phases fixed as one would in practice; see the Supplementary Information for a detailed discussion.) We stress that this result applies also in the physically relevant case where gates transport the Majoranas while the superconducting phases remain fixed; we have merely used our freedom to deform the Hamiltonian to expose the answer with minimal formalism. Furthermore, because Fig. 3e–h also represents a counterclockwise exchange, it is natural to expect the same result for this case. The Supplementary Information analyses both types of exchanges from a complementary perspective (and when the superconducting phases are held fixed), confirming their equivalence. There we also establish rigorously that in networks supporting arbitrarily many Majoranas exchange is implemented by a set of unitary operators U_{ij} analogous to those in a 2D $p+ip$ superconductor. (The Methods section outlines the analysis.) Thus the statistics is non-Abelian as advertised.

Discussion

The keyboard of gates shown in Fig. 2 and the T-junction of Fig. 3 provide the basic elements allowing manipulation of topological qubits in semiconducting wires. In principle, a single T-junction can

support numerous well-separated Majorana modes, each of which can be exchanged with any other. (First, create many Majoranas in the horizontal wire of the T-junction. To exchange a given pair, shuttle all intervening Majoranas down to the end of the vertical wire and then carry out the exchange using the methods of Fig. 3.) However, networks consisting of several T-junctions—such as the set-up of Fig. 4a—enable more efficient Majorana exchange. In the figure, all adjacent Majorana fermions can be immediately swapped using Fig. 3, whereas non-adjacent Majoranas can be shuttled down to the lower wire to be exchanged. This 'ladder' configuration straightforwardly scales up by introducing extra 'rungs' and/or 'legs'.

As Fu and Kane suggested in the topological insulator context[13], fusing Majorana fermions across a Josephson junction provides a readout method for the topological qubit states. We illustrate the physics with the schematic set-up of Fig. 4b, which extends the experiments proposed in refs 21,22 to allow the Majorana fusion rules to be directly probed. Here a semiconducting wire bridges two *s*-wave superconductors with initial phases $\varphi_{L/R}{}^i$; we assume $\Delta\varphi^i \equiv \varphi_L{}^i - \varphi_R{}^i \neq \pi$. Three gates drive the wire from an initially non-topological ground state into a topological phase. Importantly, the order in which one applies these gates qualitatively affects the physics. As we now discuss, only in the left path of Fig. 4b can the qubit state at the junction be determined in a single measurement.

Consider first germinating Majorana fermions γ_1 and γ_2 by applying the left gate. Assuming $f_A = (\gamma_1 + i\gamma_2)/2$ initially costs finite energy as γ_1 and γ_2 separate, the system initializes into a ground state with f_A unoccupied. Applying the central and then right gates shuttles γ_2 to the other end (see the left path of Fig. 4b). As a narrow insulating barrier separates the superconductors, an ordinary fermion $f_B = (\gamma_3 + i\gamma_4)/2$ arises from two coupled Majoranas $\gamma_{3,4}$ at the junction. Similar to equation (6), the energy of this mode is well-captured by[21–23] $H_J \sim i\epsilon^i\gamma_3\gamma_4 = \epsilon^i(2f_B{}^\dagger f_B - 1)$, where $\epsilon^i = \delta\cos(\Delta\varphi^i/2)$ with non-universal δ. The system has been prepared in a ground state, so the f_B fermion will be absent if $\epsilon^i > 0$ but occupied otherwise.

Suppose we now vary the phase difference across the junction away from its initial value to $\Delta\varphi$. The measured Josephson current (see Supplementary Information for a pedagogical derivation) will then be

$$I = \frac{2e}{\hbar}\frac{dE}{d\Delta\varphi} = \frac{e\delta}{\hbar}\mathrm{sgn}(\epsilon^i)\sin(\Delta\varphi/2) + I_{2e} \qquad (7)$$

where E is the ground-state energy and I_{2e} denotes the usual Cooper-pair-tunnelling contribution. The first term on the right reflects single-electron tunnelling originating from the Majoranas $\gamma_{3,4}$. This 'fractional' Josephson current exhibits 4π periodicity in $\Delta\varphi$, but 2π periodicity in the initial phase difference $\Delta\varphi^i$.

The right path in Fig. 4b yields very different results, reflecting the nontrivial Majorana fusion rules. Here, after creating $\gamma_{1,2}$, one applies the rightmost gate to nucleate another pair $\gamma_{3,4}$. Assuming f_A and f_B defined as above initially cost finite energy, the system initializes into the ground state $|0,0\rangle$ satisfying $f_{A/B}|0,0\rangle = 0$. Applying the central gate then fuses γ_2 and γ_3 at the junction. To understand the outcome, it is useful to re-express the ground state in terms of $f_A{}' = (\gamma_1 + i\gamma_4)/2$ and $f_B{}' = (\gamma_2 + i\gamma_3)/2$. In this basis $|0,0\rangle = (|0',0'\rangle - i|1',1'\rangle)/\sqrt{2}$, where $f'_{A,B}$ annihilate $|0',0'\rangle$ and $|1',1'\rangle = f_A{}'^\dagger f_B{}'^\dagger|0',0'\rangle$. Following our previous discussion, $f_B{}'$ acquires finite energy at the junction, lifting the degeneracy between $|0',0'\rangle$ and $|1',1'\rangle$. Measuring the Josephson current then collapses the wavefunction with 50% probability onto either the ground state, or an excited state with an extra quasiparticle localized at the junction. In the former case equation (7) again describes the current, whereas in the latter case the fractional contribution simply changes sign.

In more complex networks, such as that of Fig. 4a, fusing the Majoranas across a Josephson junction—and in particular measuring the sign of the fractional Josephson current—similarly allows qubit readout. Alternatively, the interesting recent proposal of Hassler *et al.*[26] for reading qubit states via ancillary non-topological flux qubits can be adapted to these setups (and indeed was originally discussed in terms of an isolated semiconducting wire[26]).

To conclude, we have introduced a surprising new venue for braiding, non-Abelian statistics, and topological quantum information processing—networks of one-dimensional semiconducting wires. From a fundamental standpoint, the ability to realize non-Abelian statistics in this setting is remarkable. Perhaps even more appealing, however, are the physical transparency and experimental promise of our proposal, particularly given the feats already achieved in ref. 35. Although topological quantum information processing in wire networks requires much experimental progress, observing the distinct fusion channels characteristic of the two paths of Fig. 4b would provide a remarkable step en route to this goal. And ultimately, if braiding in this setting can be supplemented by a $\pi/8$ phase gate and topological charge measurement of four Majoranas, wire networks may provide a feasible path to universal quantum computation[6,27–30].

Methods

In the Supplementary Information we provide a rigorous, systematic derivation of non-Abelian statistics of Majorana fermions in wire networks, thus establishing a solid mathematical foundation for the results obtained in the main text. As the analysis is rather lengthy, here we briefly outline the approach. We first define the many-body ground states in the presence of arbitrarily many Majorana fermions in an arbitrary wire network. We then establish three important general results that greatly facilitate the derivation of non-Abelian statistics. (1) If two Majoranas are exchanged without disturbing any other Majoranas in the network, all of these other Majoranas simply 'factor out' in the sense that their presence in no way affects how the degenerate ground states transform. (2) If we know how a given pair of Majoranas transforms under exchange in some minimal setting, then the same transformation holds when arbitrarily many extra Majoranas are introduced, provided they are far from those being exchanged. These first two properties are rather natural and follow from the locality of the Majorana wavefunctions. (3) The transformation of the degenerate ground states under exchange (up to an overall non-universal phase) can be deduced solely by understanding how the Majorana operators transform. This provides an enormous simplification, as it distills the problem down to understanding the behaviour of the single-body Majorana operators being braided.

It follows from these results that to understand non-Abelian statistics in wire networks composed of trijunctions, it suffices to deduce how the Majorana operators transform under the two types of braids shown in Fig. 3. We subsequently analyse these exchanges (when the superconducting phases are held fixed, as would be the case in practice) and show that the operators transform similarly to vortices in a 2D $p+ip$ superconductor, thereby establishing non-Abelian statistics. Interestingly, the picture we develop in the Supplementary Information closely resembles Ivanov's construction for non-Abelian statistics of vortices, despite their absence in wire networks. Very crudely, as the Majorana fermions move along the network to be exchanged, the effective *p*-wave superconducting phases they 'feel' vary, in loose analogy to what happens when Majorana fermions bound to vortices braid one another.

It is also interesting to note that it is not only the clockwise versus counterclockwise nature of the braid that determines how the Majorana operators transform, unlike in a 2D $p+ip$ superconductor. In addition to the handedness, the superconducting phases of the wires forming the junction also play a critical role in governing the outcome of an exchange. For example, a counterclockwise exchange with a given set of superconducting phases can have the same effect as a clockwise exchange when the superconducting phases are modified. Thus, wire networks feature more available 'knobs' that one can tune to control how an exchange impacts qubit states, which may have useful applications.

Received 29 June 2010; accepted 22 December 2010; published online 13 February 2011

References

1. Kitaev, A. Fault-tolerant quantum computation by anyons. *Ann. Phys.* **303,** 2–30 (2003).
2. Freedman, M. H. P/NP, and the quantum field computer. *Proc. Natl Acad. Sci. USA* **95,** 98–101 (1998).

3. Freedman, M. H., Kitaev, A., Larsen, M. J. & Wang, Z. Topological quantum computation. *Bull. Am. Math. Soc.* **40,** 31–38 (2003).
4. Das Sarma, S., Freedman, M. & Nayak, C. Topologically protected qubits from a possible non-Abelian fractional quantum Hall state. *Phys. Rev. Lett.* **94,** 166802 (2005).
5. Bonderson, P., Freedman, M. & Nayak, C. Measurement-only topological quantum computation. *Phys. Rev. Lett.* **101,** 010501 (2008).
6. Nayak, C., Simon, S. H., Stern, A., Freedman, M. & Das Sarma, S. Non-Abelian anyons and topological quantum computation. *Rev. Mod. Phys.* **80,** 1083–1159 (2008).
7. Leinaas, J. M. & Myrheim, J. On the theory of identical particles. *Nuovo Cimento Soc. Ital. Fis. B* **37B,** 1–23 (1977).
8. Fredenhagen, K., Rehren, K. H. & Schroer, B. Superselection sectors with braid group statistics and exchange algebras. *Commun. Math. Phys.* **125,** 201–226 (1989).
9. Fröhlich, J. & Gabbiani, F. Braid statistics in local quantum theory. *Rev. Math. Phys.* **2,** 251–353 (1990).
10. Read, N. & Green, D. Paired states of fermions in two dimensions with breaking of parity and time-reversal symmetries and the fractional quantum Hall effect. *Phys. Rev. B* **61,** 10267–10297 (2000).
11. Ivanov, D. A. Non-Abelian statistics of half-quantum vortices in *p*-wave superconductors. *Phys. Rev. Lett.* **86,** 268–271 (2001).
12. Moore, G. & Read, N. Nonabelions in the fractional quantum Hall effect. *Nucl. Phys. B* **360,** 362–396 (1991).
13. Fu, L. & Kane, C. L. Superconducting proximity effect and Majorana fermions at the surface of a topological insulator. *Phys. Rev. Lett.* **100,** 096407 (2008).
14. Linder, J., Tanaka, Y., Yokoyama, T., Sudbø, A. & Nagaosa, N. Unconventional superconductivity on a topological insulator. *Phys. Rev. Lett.* **104,** 067001 (2010).
15. Sau, J. D., Lutchyn, R. M., Tewari, S. & Das Sarma, S. Generic new platform for topological quantum computation using semiconductor heterostructures. *Phys. Rev. Lett.* **104,** 040502 (2010).
16. Alicea, J. Majorana fermions in a tunable semiconductor device. *Phys. Rev. B* **81,** 125318 (2010).
17. Sato, M. & Fujimoto, S. Topological phases of noncentrosymmetric superconductors: Edge states, Majorana fermions, and non-Abelian statistics. *Phys. Rev. B* **79,** 094504 (2009).
18. Lee, P. A. Proposal for creating a spin-polarized $p_x + ip_y$ state and Majorana fermions. Preprint at http://arxiv.org/abs/0907.2681 (2009).
19. Ghosh, P., Sau, J. D., Tewari, S. & Das Sarma, S. Non-Abelian topological order in noncentrosymmetric superconductors with broken time-reversal symmetry. *Phys. Rev. B* **82,** 184525 (2010).
20. Qi, X-L., Hughes, T. L. & Zhang, S-C. Chiral topological superconductor from the quantum Hall state. *Phys. Rev. B* **82,** 184516 (2010).
21. Lutchyn, R. M., Sau, J. D. & Das Sarma, S. Majorana fermions and a topological phase transition in semiconductor–superconductor heterostructures. *Phys. Rev. Lett.* **105,** 077001 (2010).
22. Oreg, Y., Refael, G. & von Oppen, F. Helical liquids and Majorana bound states in quantum wires. *Phys. Rev. Lett.* **105,** 177002 (2010).
23. Kitaev, A. Y. Unpaired Majorana fermions in quantum wires. *Phys.-Usp.* **44,** 131–136 (2001).
24. Wimmer, M., Akhmerov, A. R., Medvedyeva, M. V., Tworzydło, J. & Beenakker, C. W. J. Majorana bound states without vortices in topological superconductors with electrostatic defects. *Phys. Rev. Lett.* **105,** 046803 (2010).
25. Fu, L. & Kane, C. L. Josephson current and noise at a superconductor/quantum-spin-Hall-insulator/superconductor junction. *Phys. Rev. B* **79,** 161408(R) (2009).
26. Hassler, F., Akhmerov, A. R., Hou, C-Y. & Beenakker, C. W. J. Anyonic interferometry without anyons: How a flux qubit can read out a topological qubit. *New J. Phys.* **12,** 125002 (2010).
27. Bravyi, S. & Kitaev, A. Universal quantum computation with ideal Clifford gates and noisy ancillas. *Phys. Rev. A* **71,** 022316 (2005).
28. Freedman, M., Nayak, C. & Walker, K. Towards universal topological quantum computation in the $\nu = 5/2$ fractional quantum Hall state. *Phys. Rev. B* **73,** 245307 (2006).
29. Bonderson, P., Das Sarma, S., Freedman, M. & Nayak, C. A blueprint for a topologically fault-tolerant quantum computer. Preprint at http://arxiv.org/abs/1003.2856 (2010).
30. Bonderson, P., Clarke, D. J., Nayak, C. & Shtengel, K. Implementing arbitrary phase gates with Ising anyons. *Phys. Rev. Lett.* **104,** 180505 (2010).
31. Dresselhaus, G. Spin–orbit coupling effects in zinc blende structures. *Phys. Rev.* **100,** 580–586 (1955).
32. Bychkov, Y. A. & Rashba, E. I. Oscillatory effects and the magnetic susceptibility of carriers in inversion layers. *J. Phys. C* **17,** 6039–6045 (1984).
33. Winkler, R. *Spin–Orbit Coupling Effects in Two-Dimensional Electron and Hole Systems* (Springer, 2003).
34. Stern, A., von Oppen, F. & Mariani, E. Geometric phases and quantum entanglement as building blocks for non-Abelian quasiparticle statistics. *Phys. Rev. B* **70,** 205338 (2004).
35. Doh, Y-J., van Dam, J. A., Roest, A. L., Bakkers, E. P. A. M., Kouwenhoven, L. P. & De Franceschi, S. Tunable supercurrent through semiconductor nanowires. *Science* **309,** 272–275 (2005).

Acknowledgements

We have benefited greatly from stimulating conversations with P. Bonderson, S. Das Sarma, L. Fidkowski, E. Henriksen, A. Kitaev, P. Lee, X. Qi and A. Stern. We also gratefully acknowledge support from the Lee A. DuBridge Foundation, ISF, BSF, DIP and SPP 1285 grants, Packard and Sloan fellowships, the Institute for Quantum Information under NSF grants PHY-0456720 and PHY-0803371, and the National Science Foundation through grant DMR-0529399.

Author contributions

All authors contributed to the inception of the ideas in the manuscript, design of networks and proposed experimental setups, and proof of non-Abelian statistics.

Additional information

The authors declare no competing financial interests. Supplementary information accompanies this paper on www.nature.com/naturephysics. Reprints and permissions information is available online at http://npg.nature.com/reprintsandpermissions. Correspondence and requests for materials should be addressed to J.A.